Design and Fabrication of a High-Performance Magnetic Actuator for Magnetic Pulse Welding of Metal Tubes with Large Diameters

Xiaoxiang Li, Quanliang Cao, Zhipeng Lai, Yiliang Lv, Siyuan Chen, Yi zhang, Xiaotao Han, and Liang Li

Abstract Magnetic pulse welding (MPW) is a high-speed joining process that uses pulse electromagnetic force to achieve welding. It is a clean welding process and it can be applied to dissimilar metals welding, which has a wide range of application prospects. However, this technology is currently mainly used for welding small-diameter thin-walled tubes. This is because the energy and electromagnetic force required for welding increase significantly as the tube size increases, which consequently places strict requirements on welding tools, including pulsed power and coil. To solve this issue, this work developed a two-dimensional (2D) axial-symmetry finite element model to optimize the tube welding process and designed a high-performance magnetic actuator with a high-strength coil to generate a strong enough electromagnetic force. On this basis, both numerical and experimental studies were performed to investigate the welding behavior of a 6061 aluminum alloy tube and a 304 stainless steel tube with 110 mm diameter and 3 mm thickness. Finally, a mechanical test and scanning electron microscope (SEM) were used to verify the joining quality, and the results show that the metallurgical bonding occurred between the two tubes. The presented optimization method and tool design could be of significance to the practical applications of MPW technology.

Keywords Magnetic pulse welding · Tube welding · Dissimilar metals welding · Large diameter tube

X. Li · Q. Cao · Z. Lai · Y. Lv · S. Chen · Y. zhang · X. Han · L. Li (✉)
Wuhan National High Magnetic Field Center, Huazhong University of Science and Technology, Wuhan 430074, China
e-mail: liangli44@hust.edu.cn

State Key Laboratory of Advanced Electromagnetic Engineering and Technology, Huazhong University of Science and Technology, Wuhan 430074, China

1291

1   Introduction

Magnetic pulse welding (MPW) is an advanced and clean technology, which can translate electric power into kinetic energy of metallic tubes or sheets and achieve welding by high-speed impact. Compared with traditional fusion welding, MPW is a kind of solid-state welding process. Without an obvious welding seam, the shortcoming of a heat-affected area can be avoided. In addition, the joining of dissimilar materials is impossible for the conventional fusion welding process due to huge differences in melting point, thermal conductivity, volumetric specific heat, and coefficient of thermal expansion [1]. As MPW can achieve atomic diffusion of two materials by high-speed impact, this method can be used to join dissimilar materials and achieve lighter and stronger material combinations. Other high-speed welding technologies, like explosive welding, laser impact welding, and vaporizing foil actuator welding are mainly applied to sheet welding. MPW has significant advantages in tube welding because of the axisymmetric structure of the coil actuator.

At present, MPW technology is mainly used for tubes with a diameter of less than 50 mm and thickness thinner than 1 mm, like automotive space frame and cable connector, as in [2]. To the best of our knowledge, the largest diameter of magnetic tube welding research latest reported is 80 mm [3]. Welding large and thick tubes needs more input energy to generate high driving pressures between magnetic actuator and tubes in a short acceleration time. The lack of high-energy power supplies or the low efficiency of welding actuators makes the energy input unsatisfactory. Furthermore, high driving pressures can also lead to shorten the longevity of the actuator or even damage the equipment which makes it difficult to weld large diameter tubes [4]. To solve these problems, a necessary task is to optimize the welding system via an effective simulation model, which can be used to improve the utilization of magnetic energy. As the MPW system is not a perfect two-dimensional axial-symmetry system, the existing simulation models are mainly based on the 3D model [5, 6]. Although these models can analyze the whole MPW process accurately, it is complex and low efficiency to achieve optimization work. Yu et al. 2005 established a 2D model by ANSYS to explore the effect of field shaper on magnetic pressure distribution in electromagnetic modules [7]. But the MPW is a multi-physics coupling process and the optimization of detailed parameters of magnetic actuators is rarely mentioned. In addition to optimization work, how to increase the structural strength of the coils used in the MPW process is also critical, which is the key to ensuring that a sufficiently strong electromagnetic force can be generated. In this regard, our group has done some related research. For example, the high-field pulsed magnet manufacturing technology has been introduced to increase the coil strength in the field of electromagnetic forming [8]. A new discharge circuit configuration with a crowbar circuit was proposed to reduce the Joule heating of the coil [9]. A dual-coil system was developed to improve the forming ability of sheet and tube processing [10, 11].

This paper provides an effective two-dimensional model for the optimization of design of the MPW process by simplifying the boundary conditions in COMSOL.

Aiming at welding aluminum tubes with 110 mm diameter and 3 mm thickness, the effects of actuator parameters such as the coil turns and the structural parameters of the field shaper on the magnetic pressure are analyzed in detail, and a high-strength coil has been designed and fabricated. Furthermore, a variable-size, multi-function MPW experimental platform is developed and a series of experiments are carried out to achieve the high-quality welding between the AA6061 and SS304 tubes. Finally, some mechanical and metallography tests are performed to evaluate the welding quality.

2 Simulation

For tube welding, a magnetic actuator is placed outside the two tubes and energized with a capacitor bank. The interaction between the generated magnetic field and the induced eddy current in the outer metal tube will trigger a strong Lorentz force that induces the high-speed impact of two tubes, as shown in Fig. 1a. Field shaper (FS) is an important part that has an effect on the distribution of the magnetic field. The magnetic actuator is not a perfect two-dimensional axial symmetry model and a slot exists in the FS. Through this slot structure, the magnetic field generated by the coil can access the area near the outer tube, as shown in Fig. 1b. In the FS region, the slot cuts off the current in the hoop direction, and the FS can be regarded as a single-turn secondary coil [12]. In COMSOL software, the model can be treated as a 2D axial symmetry model by defining the FS region as a coil characteristic and making its total current to zero all the time.

A 2D axial symmetry finite element simulation model has been built by the COMSOL Multiphysics software package. In the time domain, five physical modules are solved by the unity coupling mode: (1) the "global ordinary differential equations (ODEs) and differential algebraic equations (DAEs)" module; (2) the "magnetic fields" module; (3) the "solid mechanics" module; (4) the "Heat transfer in solid"
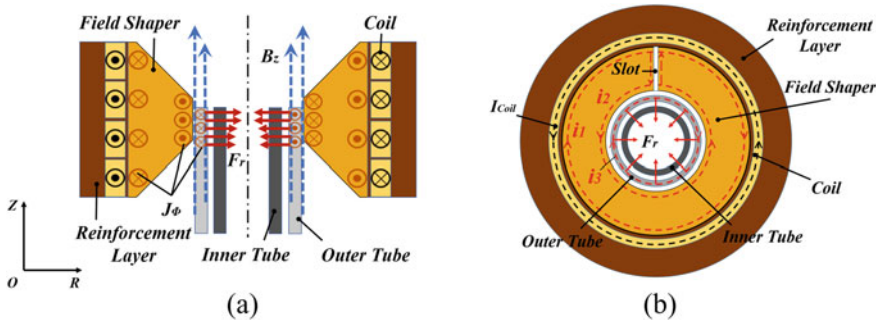
Fig. 1 Schematic diagram of the MPW process: **a** The front view and **b** the top view. (Color figure online)
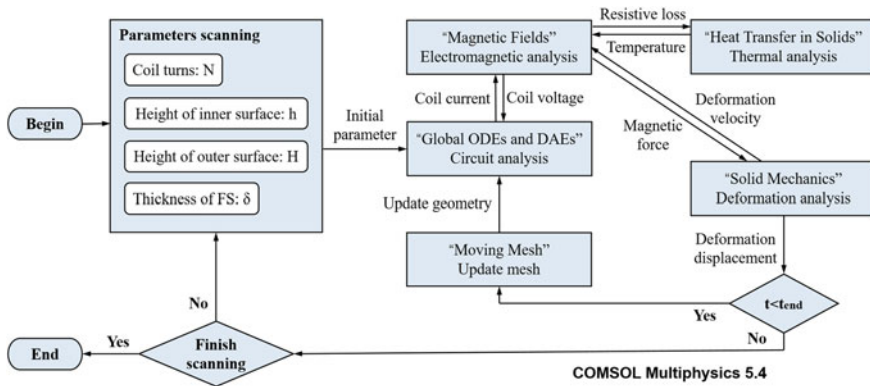
**Fig. 2** Flowchart of the implemented algorithm. (Color figure online)

module; and (5) the "moving mesh" module. A flowchart of the simulation process is shown in Fig. 2.

Higher impact velocity means more likely to achieve welding in MPW. The maximization of impact velocity of the outer tube is regarded as an optimization objective. COMSOL has an outstanding ability to solve multi-physics coupling problems and very convenient to use its built-in optimized model. As the simulation model is based on the finite element method (FEM), the air region is required to calculate the electromagnetic field and to define the boundary of the whole area. Considering the air mesh will be distorted when solving the above coupling physical fields, the "Moving Mesh" model is applied to update and redraw the air mesh to ensure high-precision simulation. Note that the air resistance was not considered in this optimization design model. To get the optimized parameters, combining the results of magnetic pressure calculated by "magnetic fields" model and the velocity which is calculated by "solid mechanics" model can be more convincing. The diagram of mesh subdivision is shown in Fig. 3. The magnetic pressure represents the magnetic field energy density, which can be calculated by Eq. (1) based on the magnetic field intensity near the tube:

$$p_m(t) = \frac{1}{2}\mu\left(H_o^2(t) - H_i^2(t)\right) \tag{1}$$

where H_o represents the magnetic field intensity between FS and tube, and H_i represents the field intensity inside the tube [13]. The second method is to take the line integral of the Lorentz force on the wall thickness of the workpiece, as shown in Eq. (2):

$$p_m(t) = \int_{r_{in}}^{r_{out}} f_m(r, t) dr \tag{2}$$
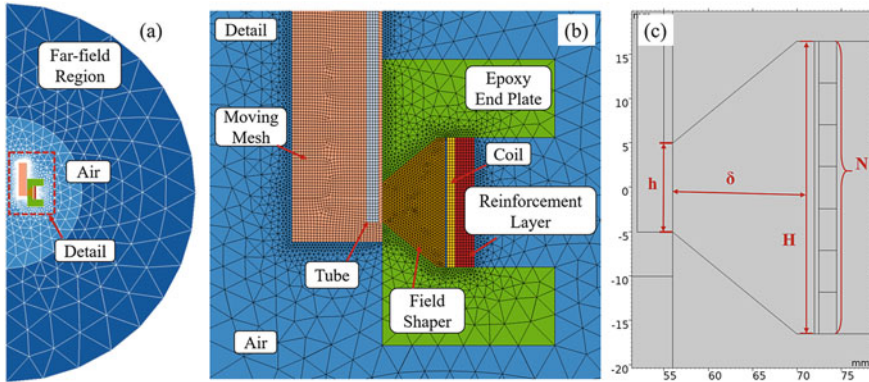
Fig. 3 Finite element mesh for the MPW system and a schematic diagram of the simulation model. (Color figure online)

where f_m represents the Lorentz force, r_{in} and r_{out} are the inner and outer diameter of the tube, respectively. The two methods mentioned above are both feasible. As this paper mainly analyzes the velocity of the tube end, the second method was adopted.

3 Experiment

3.1 Experimental Configuration

The actuator with optimized parameters is made according to the simulation results. Figure 4 shows the experimental configuration. An aluminum alloy tube (AA6061) with a diameter of 110 mm and thickness of 3 mm was welded to steel tubes with
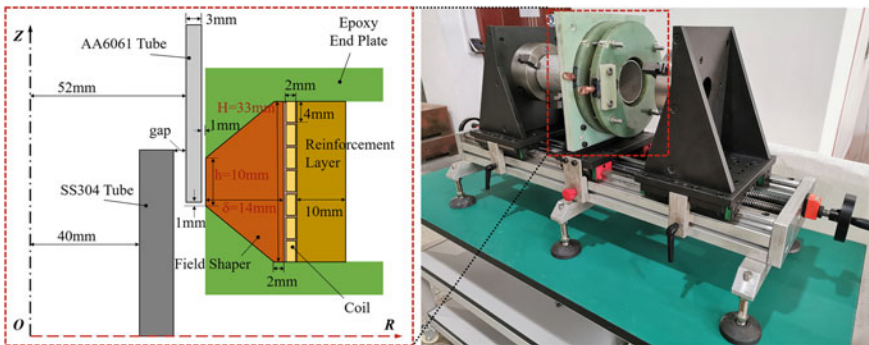
Fig. 4 Geometric model of the experimental configuration and experimental platform. (Color figure online)

different diameters. In order to improve the magnetic energy utilization, the multi-turn coil structure was chosen and the field shaper was by copper wires with rectangular cross-section directly. The copper wires were covered with polyimide film to ensure a high degree of insulation between turns. This design makes the distance between the coil and the field shaper only 0.5 mm, and reduces the stray losses significantly. In addition, decreasing the length of the overlap between the tube and the FS working area can reduce the non-effective connection [14]. In the experiment and optimization design, there is an uncovered distance between the end of the tube and the inner surface edge of the FS along the axial direction to enhance the electromagnetic force, and the distance is set to 1 mm. The reinforcement layers are very important for improving the strength of the coil. High-tensile strength material (Zylon) was used to increase the strength of the reinforcement. The detailed system parameters are shown in Table 1.

To adapt to tubes with different diameters, two three-jaw chucks were used to fix the outer and inner tubes. And the actuator was coaxially placed with two three-jaw chucks. The horizontal position of chucks is controlled by two screw rods with a position indicator. This design makes the repetitive experiment of different-sized tubes become realizable. Our laboratory, the Wuhan National High Magnetic Field Center, has developed several sets of pulse capacitance supplies for MPW, and the parameters of the discharge circuit are shown in Table 2.

Table 1 System parameters used in this experiment

Parameters	Description	Value
Coil (Copper conductor)		
ρ_c	Mass density	8.9×10^3 kg/m^3
E_c	Young's modulus	110 GPa
v_c	Poisson's radio	0.34
σ_{y0c}	Initial yield stress	135 MPa
E_c^T	Tangent modulus	0.4 GPa
Reinforcement (Zylon fiber)		
ρ_z	Mass density	1.56×10^3 kg/m^3
E_z	Young's modulus	3/230/3 GPa
v_z	Poisson's radio	0.34/0.0148/0.0148
Coil frame (Epoxy resin board)		
ρ_e	Mass density	2.6×10^3 kg/m^3
v_e	Young's modulus	22 GPa
E_e	Poisson's radio	0.34
Stycast W19		
ρ_s	Mass density	2.4×10^3 kg/m^3
E_s	Young's modulus	22 GPa
v_s	Poisson's radio	0.34

Table 2 System parameters used in this experiment

| Parameter	Description	Value/category
C	Capacitance	150 μF
L_l	Line inductance	2.6 μH
R_l	Line resistance	18 mΩ
U_c	Charging voltage	0–20 kV
S	Switch	Self-breaking spark gap switch

3.2 Experimental Design

First, a series of discharge experiments were performed to explore how the discharge voltage and accelerate gap influence the welding quality. The discharge voltages range from 8 to 17 kV for the interval 1 kV. The gap distances between the two tubes range from 2 to 6.5 mm, and the interval is 1.5 mm. Since the surface treatment of the two tubes has a significant impact on the mechanical properties of weldments [15], the roughness of the outer surface of the steel tube was controlled at 0.65 ± 0.15 μm. During the welding process, the discharge voltages and currents were measured by a high-voltage probe and a Rogowski coil. After discharge experiments, the weldment was processed to mechanical testing samples by wire-electrode cutting. Peel tests and tensile tests were used to evaluate the quality of joining. Finally, scanning electron microscopy (SEM) is used to observe the distribution of elements. The results can be used to judge whether the metallurgical bonding occurs between the two dissimilar materials tubes.

4 Results and Discussion

4.1 Distribution of Magnetic Pressure and Stress

Figure 5a shows the current and voltage curves of the coil from discharge voltage to be 15 kV. The experimental curves are consistent with simulation results, demonstrating that the simulations accurately reflected the experimental process. The distribution of magnetic field and pressure is shown in Fig. 5b. FS can concentrate the pressure on the tube surface effectively and the distribution of pressure is the same as the results calculated by Yu et al. [7]. As the maximum discharge capacity of our equipment is 20 kV, the von Mises stress in the radial direction of the coil and reinforce parts were calculated at 20 kV situation. The results are shown in Fig. 5c. The coil is reinforced by Zylon fiber composite, whose ultimate tensile strength is about 3.5 GPa. When the thickness of the reinforcement is 10 mm, the maximum von Mises stress in the Zylon is 3.5 GPa. In practice, the maximum discharge voltage of our experiments is 17 kV, lower than the maximum discharge voltage. So, the 10 mm thickness of the reinforcing layer to ensure safety is enough.
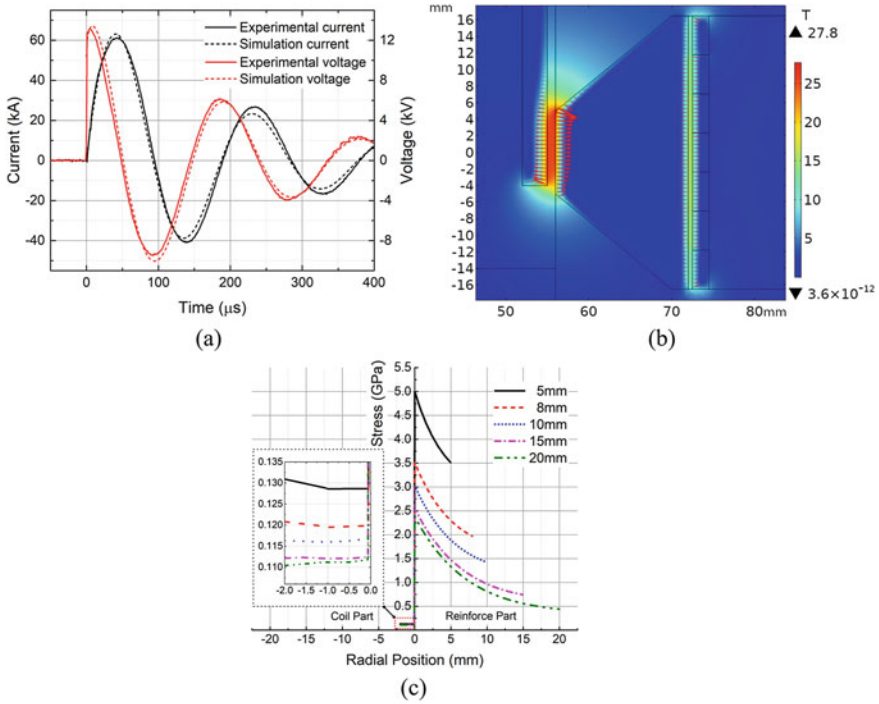
Fig. 5 Simulation results: **a** current and voltage curves compared with experimental results, **b** the distributions of magnetic field and pressure, and **c** the von Mises stress of coil and reinforce parts. (Color figure online)

4.2 Optimization Results of Coil and FS

The optimal results of coil turns N, height of FS inner surface h, height of FS outer surface H, and FS thickness δ are presented in Fig. 6. The velocity and pressure increase first and then decreases with increasing coil turns N can be found in Fig. 6a. According to Biot-Savart law, it can be derived that the magnetic flux density B is proportional to ampere-turns NI. As coil current I decreased with N increasing, there is a maximum value of NI and B. Figure 6b presents that magnetic pressure and velocity are monotonically decreasing with the height of inner surface h. It can be explained that the smaller the inner surface is, the magnetic field can be more concentrated. However, the welding area should not be too small for comprehensive consideration, and $h = 10$ mm was selected.

To explore the universal laws of the size effect, the ratios of FS thickness and outer surface height to inner surface height are defined as two coefficients to reflect the relative dimension. The influence of the coefficient of the thickness ($k_\delta = \delta/h$) and the outer surface height ($k_H = H/h$) both have the same variation trend, which is increased first and then decreased, as shown in Fig. 6c, d. It is speculated that this
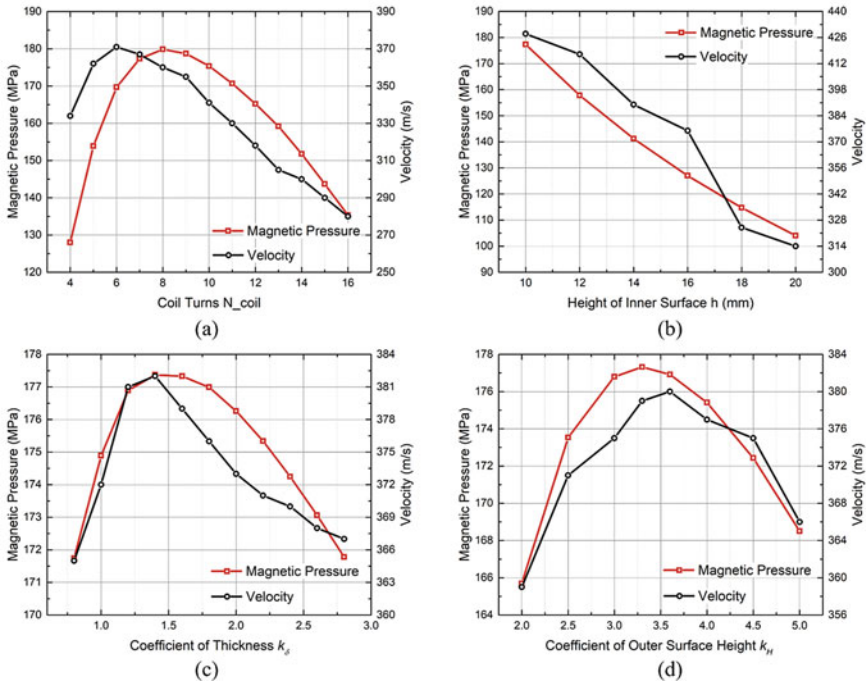
Fig. 6 Magnetic pressure and velocity variation curves with **a** coil turns, **b** height of inner surface, **c** coefficient of thickness, and **d** coefficient of outer surface height. (Color figure online)

change in trend is related to the energy utilization rate. The change of FS thickness and outer surface height leads to variety of impedance and inductive reactance of the load. As the energy is consumed in the circuit part and load part, this variety will affect the energy transformation ratio eventually.

For synthesis, considering the optimal results of magnetic pressure and velocity, the parameters of coil and FS were chosen finally. The details are shown in Fig. 4.

4.3 Mechanical Testing and Welding Windows

The results of welding characteristics and quality were obtained by peel testing and tensile test. According to the tensile test methods on the weld and deposited metal (GB/T 2652-2008), the tensile samples were designed and processed by wire-electrode cutting. As the welding joint is thick and long (both more than 10 mm), it is difficult to keep the direction of tensile force on a fixed line, and therefore two improvement measures were carried out. First, a metal block with a thickness of steel tube was placed on the aluminum side, while another metal block with a thickness of aluminum tube was placed on the steel side. Second, an epoxy splint was used

to avoid the bending of samples' working areas. Considering the influence of the FS slot, two positions of weldment of each tube were tested: the positions near or opposite the slot of the FS. And the results of characteristics can be classified into three types: (1) No falling off at two positions, the situation was regarded as **fully weld**, (2) only one position bonding, the situation was regarded as **part weld**, (3) both two positions falling off, this situation was regarded as **no weld**.

Further, the tensile test was done on fully weld samples to evaluate the welding quality. If a sample fracture at the base material or the tensile force is greater than 3200 N (corresponding to 90 MPa stress), it can be regarded that the strength of the weldment is stronger than the aluminum base material, and it can be defined as a high-strength combination. If the fracture occurs at the weld joint and the tensile force is less than 3200 N, it means that the strength of the weldment failed to obtain promotion.

Considering the results of the two positions as mentioned above, the welding quality can be divided into three categories: (1) when high-strength combination occurs at two positions, the situation is regarded as **high-quality weld**, (2) when high-strength combination occurs at only one position, this situation is regarded as **medium-quality weld**, (3) when no high-strength combination occurs at these two positions, the situation is regarded as **low-quality weld**. The welding window of a large diameter metal tube was obtained and drawn in Fig. 7. The results show that there are some differences and correlations between welding boundary and high-quality welding boundary.

For each fixed gap, an increasing voltage can improve the welding quality. As the radial deformation is fixed, the energy lost to overcome the deformation of the material is the same. So, more energy input from the actuator means more kinetic energy can be translated into the outer tube. Higher impact velocity makes it easier to achieve welding and improve the welding quality. Moreover, both welding boundary and high-quality welding boundary have optimal welding gap and lowest discharge
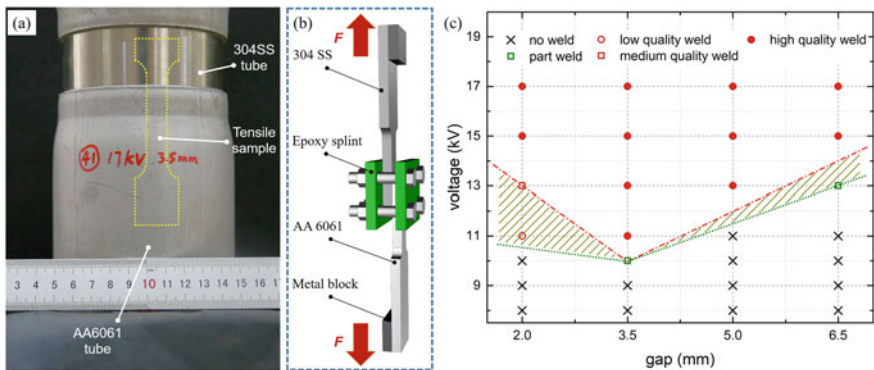

Fig. 7 The welding window of large diameter metal tubes: **a** The result of 17 kV voltage and 3.5 mm gap discharge conditions, **b** schematic diagram of tensile test, and **c** welding window. (Color figure online)

voltage. It is supposed that when the gap distance is small, increasing the gap can increase the acceleration space so that more kinetic energy can be loaded on the metal tube. As the gap continues to increase, more energy is needed to overcome the plastic deformation of the tube, resulting in the reduction of kinetic energy.

4.4 Metallographic Analysis

The test results of the welding sample using SEM and energy dispersive spectrum (EDS) under the conditions of 17 kV discharge voltage and 3.5 mm gap distance are shown in Fig. 8. It can be clearly found that the diffusion process occurred between Al and Fe. As a result, an obvious element transition layer is formed at the weldment area. Also, the dimension of the transition layer is about 10 μm. Considering the SEM image of the interlayer characteristics, the temperature was enough to melt the whole interface due to the high collision velocity under this discharge condition [16]. A large volume of mixtures of Al and Fe were formed at the interface under the high-pressure condition. These results demonstrate the metallurgical bonding occurring between the two dissimilar materials tubes.
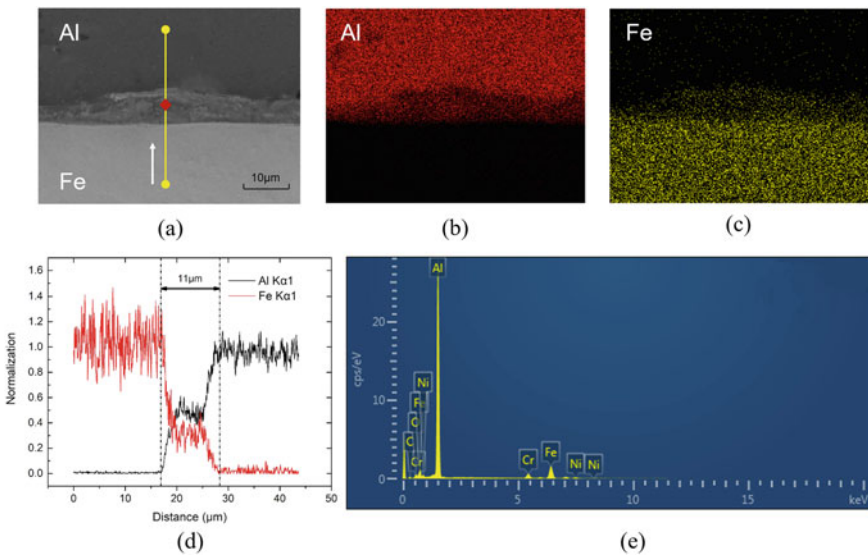
Fig. 8 Pictures of **a** SEM photo, **b** distribution of Al atoms, **c** distribution of Fe atoms, **d** EDS line results, and **e** EDS spot results. (Color figure online)

5 Conclusions

In this paper, the optimal design and experimental study for magnetic pulse welding of dissimilar metal tubes with large diameters were analyzed in detail. Some conclusions can be summarized as follows:

(1) An effective two-dimensional simulation model for the optimization of the design of MPW was built by COMSOL, and the results obtained from the simulations are consistent with the experimental observations, providing an efficient approach for MPW system design.
(2) Some optimization parameters were analyzed how to influence the magnetic pressure and tube velocity. These principles are helpful to understand the operating principles of the magnetic actuator and provide a practical basis for further numerical model building.
(3) By the experimental method, the welding windows of gaps and discharge voltages were built up. The experimental results also prove that the magnetic welding of tubes with 110 mm diameters and 3 mm thickness became reality, and the strength of the welding area can be stronger than the basic material.
(4) By using SEM, the element diffusion phenomenon was observed between Al and Fe. This result also demonstrates the metallurgical bonding occurring between the two dissimilar materials tubes.

References

1. Kapil A, Sharma A (2015) Magnetic pulse welding: an efficient and environmentally friendly multi-material joining technique. J Clean Prod 100:35–58
2. Weddeling C, Walter V, Haupt P, Tekkaya AE (2015) Joining zone design for electromagnetically crimped connections. J Mater Process Technol 225:240–261
3. Bellmann J, Schettler S, Dittrich S, Lueg-Althoff J, Schulze S, Hahn M, Beyer E, Tekkaya AE (2019) Experimental study on the magnetic pulse welding process of large aluminum tubes on steel rods. In: IOP conference. Materials science and engineering, vol 480, 012033
4. Vivek A, Hansen SR, Liu BC, Daehn GS (2013) Vaporizing foil actuator: a tool for collision welding. J Mater Process Technol 215:2304–2311
5. Sapanathan T, Yang K, Chernikov D, Raoelison RN, Gluschenkov V, Buiron N, Rachik M (2017) Thermal effect during electromagnetic pulse welding process. Trans Tech Publ 879:1662–1667
6. Rajak AK, Kumar R, Basumatary H, Kore SD (2018) Numerical and experimental study on effect of different types of field-shaper on electromagnetic terminal-wire crimping process. Int J Precis Eng Man 19(3):453–459
7. Yu HP, Li CF, Zhao ZH, Li Z (2005) Effect of field shaper on magnetic pressure in electromagnetic forming. J Mater Process Technol 168(2):245–249

8. Qiu L, Han XT, Peng T, Ding HF, Xiong Q, Zhou ZY, Jiang CX, Lv YL, Li L (2012) Design and experiments of a high field electromagnetic forming system. IEEE Trans Appl Supercon 22(3):3700504

9. Cao QL, Han XT, Lai ZP, Xiong Q, Zhang X, Chen Q, Xiao HX, Li L (2015) Analysis and reduction of coil temperature rise in electromagnetic forming. J Mater Process Technol 225:185–194

10. Lai ZP, Cao QL, Han XT, Huang YJ, Deng FX, Chen Q, Li L (2017) Investigation on plastic deformation behavior of sheet workpiece during radial Lorentz force augmented deep drawing process. J Mater Process Technol 245:193–206

11. Li XX, Cao QL, Lai ZP, Ouyang SW, Liu N, Li M, Han XT, Li L (2020) Bulging behavior of metallic tubes during the electromagnetic forming process in the presence of a background magnetic field. J Mater Process Technol 276:116–411

12. Kim YB, Platner ED (1959) Flux concentrator for high-intensity pulsed magnetic fields. Rev Sci Instrum 30(7)

13. Welddeling C, Demir OK, Haupt P, Tekkaya AE (2015) Analytical methodology for the process design of electromagnetic crimping. J Mater Process Technol 222:163–180

14. Lu ZY, Gong WT, Chen SJ, Yuan T, Kan CL, Jiang XQ (2019) Interfacial microstructure and local bonding strength of magnetic pulse welding joint between commercially pure aluminum 1060 and AISI 304 stainless steel. J Manuf Process 46:59–66

15. Cui JJ, Sun T, Geng HH, Yuan W, Li GY, Zhang X (2018) Effect of surface treatment on the mechanical properties and macrostructures of Al-Fe single-lap joint by magnetic pulse welding. Int J Adv Manuf Tech 98:1081–1092

16. Cui JJ, Ye L, Zhu CC, Geng HH, Li GY (2020) Mechanical and microstructure investigations on magnetic pulse welded dissimilar AA3003-TC4 joints. J Mater Eng Perform 29:712–722